Supplementary materials to:
Glacial controls on iron and manganese concentration and lability in an Arctic fjord

Łukasz Stachnik[1,2], Meri Korhonen[3], Jonathan R. Hawkings[4,5], Marlena Szeligowska[6], Katarzyna Koziorowska[6], Emilia Trudnowska[6], Karol Kuliński[6], Beata Szymczycha[6], Oskar Głowacki[3], Małgorzata Kitowska[6], Katarzyna Dragańska-Deja[6], Marcin Syczewski[2,7], Liane G. Benning[2,8], Pablo Forjanes[2], Mateusz Moskalik[3]

[1]Alfred Jahn Cold Regions Research Centre, University of Wrocław, 50-383, Wrocław, Poland
[2] GFZ, Helmholtz Centre for Geosciences, 14473, Potsdam, Germany
[3]Institute of Geophysics, Polish Academy of Sciences, Warszawa, Poland
[4]University of Pennsylvania, 19104-6316, Philadelphia, USA
[5]iC3, The Arctic University of Norway, Tromsø, Norway
[6]Institute of Oceanology Polish, Academy of Sciences, 81-712, Sopot, Poland
[7] Faculty of Biology, University of Warsaw, 02-096, Warszawa, Poland
[8] Department of Earth Sciences, Freie Universität Berlin, 12249, Berlin, Germany

Correspondence to: Lukasz Stachnik (lukasz.stachnik@uwr.edu.pl)

1 Supplementary methods

1.1 Sedimentation rate and SPM concentration from monitoring in Polish Polar Station Hornsund

In addition to the three cruises used for data collection onboard SV Azimuth, supplementary data on Suspended Particulate Matter and sedimentation rate were collected during 2022-2025 as part of oceanographic monitoring in Hornsund fjord. Observations were not continuous and sampling varied between years. On average, measurements in May covered about 4 days in Gåshamna and 7 days in Hansbukta. In July-August, on average 25 days were covered in Gåshamna and 17 days in Hansbukta. Water samples were collected with a Hydrobios Free Flow 1 l Niskin Bottle from multiple depths in the water column. The daily sedimentation rate was measured 5 m above the sea floor. The sediment traps were deployed for a minimum of 24 h, but generally daily fluxes were calculated from exposure lasting approximately 10 days. Longer exposure time resulted in the need of partitioning the 1 l sample before filtration and typically 1/4, 1/8 or 1/16 of the sample was filtered. Collection and sample treatment of these supplementary water samples were similar to SPM analysis from the yacht cruises with the difference of filter type. These samples, as well as the sediment trap samples from the yacht cruises, were filtered through Whatman GF/F filters (pore size 0.7 µm, diameter 45 mm). Prior to filtration the filters were dried in a 200 °C oven for 2 hours before weighing. After filtration the filters were dried at 40 °C for 24 hours and left in the desiccator before weighing.

1.2 Berger leach

Labile particulate Fe and Mn were additionally quantified using the Berger leach extraction following Berger et al. (2008). Particulate material collected on filters was leached with 1 mL of a weak reducing solution consisting of 25% (v/v) acetic acid and 0.02 M hydroxylamine hydrochloride, and heated in a water bath at 95 °C for 10 min, followed by equilibration at room temperature to a total leaching time of ~2 h. After removal of the filter, leachates

were centrifuged to remove residual particles, acidified with ultrapure HNO_3, evaporated to near dryness, and re-dissolved prior to analysis. This operationally defined leach targets surface-bound and easily reducible particulate metal phases without dissolving refractory silicates and has been widely applied to suspended particulate matter in riverine, coastal, and glacially influenced environments (Berger et al., 2008; Forsch et al., 2025).

1.3 Filtration, sample treatment and analysis of dissolved organic carbon (DOC), nutrients (dissolved inorganic nitrogen (DIN, expressed as the sum of nitrate (NO_3^-), nitrite (NO_2^-), ammonium (NH_4^+), dissolved phosphate (PO_4^{3-})), particulate organic carbon (POC), particulate total nitrogen (PTN) as well as stable carbon (δ^{13}C-POC) and nitrogen (δ^{15}N-PTN) isotopes composition.

Samples for dissolved inorganic macronutrient concentrations (µmol/L) were first collected into 60 mL syringes, which were then passed through a 0.45 µm cellulose acetate filter into 15 mL polypropylene Falcon tubes. Samples were kept frozen until analysis. DOC samples (22 mL) were filtered through pre-combusted MN GF-5 filters (0.4 µm), transferred to glass bottles, and acidified to pH ~2 with HCl to suppress biological activity and eliminate inorganic carbon. For particulate analysis, 1–2 L of seawater was filtered onto pre-combusted, pre-weighed MN GF-5 filters (0.4 µm). These were analysed for POC, PTN, and their stable isotope signatures (δ^{13}C and δ^{15}N). Nutrient concentrations were determined using an automated continuous-flow analyzer (e.g., SEAL AA500) following standard colorimetric protocols (Grasshoff et al., 2009). Method detection limits were approximately 0.1 µmol/L for PO_4^{3-}, 0.3 µmol/L for DSi and NO_3^-, and 0.27 µmol/L for NH_4^+, with analytical precision typically ranging from 0.01 to 0.03 µmol/L. Accuracy was verified using certified reference materials (Saghravani et al., 2024) . Dissolved inorganic nitrogen (DIN) was calculated as the sum of NO_3^-, NO_2^-, and NH_4^+. Dissolved organic carbon (DOC) concentrations were determined using high-temperature catalytic oxidation (HTCO) on a total organic carbon analyzer (e.g., Shimadzu TOC-L). Samples were combusted at ~680 °C over a platinum catalyst, and the resulting CO_2 was quantified by infrared detection. Analytical precision was typically ±4, and accuracy was verified using deep ocean reference materials, yielding recoveries of ~99%. Particulate organic carbon (POC) and total nitrogen (PTN) were measured from material collected on pre-combusted glass-fiber filters. Prior to analysis, filters were freeze-dried, weighted and homogenized, then samples were weighted into silver capsules and acidified 4 times using 2M HCl to remove carbonates. Samples were analyzed using an Elemental Analyzer Flash EA 1112 Series combined with the Isotopic Ratio Mass Spectrometer IRMS Delta V Advantage (Thermo Electron Corp., Germany). Analytical precision was better than ±0.1‰ for δ^{13}C and ±0.05‰ for δ^{15}N.

1.4 pXRD and SEM analyses

The mineralogical composition and particle morphologies and semi-quantitative chemical compositions of selected suspended particulate matter (SPM) samples were characterised by powder X-ray diffraction (pXRD) and scanning electron microscopy coupled with energy-dispersive X-ray spectroscopy (SEM-EDS). These analyses were used to identify the dominant mineral phases and to link the bulk mineral assemblage to the occurrence of fine-grained Fe-bearing particles and coatings relevant to the operationally defined labile Fe and Mn pools. For pXRD, dried SPM material was manually homogenised and powdered using an agate mortar. Diffraction patterns were collected using a STOE Stadi P diffractometer equipped with a DECTRIS MYTHEN 2 detector and a Ge(111) monochromator, using Cu radiation (lambda = 1.54 A). The samples were analysed in glass capillaries or

as flat-disc mounts, depending on the amount and physical character of the available particulate material, in order to obtain the highest possible signal-to-noise ratio and peak resolution. Mineral identification was carried out by comparing the measured diffraction patterns with reference patterns from the modified Crystallographic Open Database (COD2019) using PROFEX software. Where appropriate, semi-quantitative assessment of mineral abundances was supported using CrystalDiffract 7.0. The reference mixture used for this purpose was based on crystallographic information files (CIFs) for the main mineral phases expected in glacially derived metasedimentary SPM, including quartz, feldspar (albite), chlorite, muscovite, amphibole (hornblende), calcite, dolomite, siderite and goethite. The approach allowed comparison of the relative reflective power of individual phases and provided a semi-quantitative basis for evaluating the dominant mineral assemblages. For SEM-EDS observations in the Hornsund SPM samples, separate aliquots of water were filtered through track-etched polycarbonate Sartorius filters with a 0.22 μm pore size. Selected particles and aggregates were mounted on aluminium SEM stubs using carbon adhesive tape and carbon coated prior to analysis. The preparation and analytical workflow followed the facilities protocol used for glacial SPM mineralogical characterisation, in which particles can be re-suspended in isopropanol by sonication, drop-cast onto glass coverslips, attached to Al stubs and coated with approximately 20 nm of carbon using a Leica ACE600 EM coater. Electron microscopic imaging and semi-quantitative elemental analysis were performed using a Quanta 3D FEG scanning electron microscope (Thermo Fisher Scientific™, formerly FEI) coupled to an Octane Elect EDS detector (EDAX). SEM-EDS data were acquired at 20 kV; the reference analytical protocol used a beam current of 4 nA. The EDAX spectra were acquired with a 30 s live time, 34.6 degree take-off angle, 0.96 microsecond amplifier time and an energy resolution of approximately 129.6 eV. Elemental spectra were used as semi-quantitative indicators of particle chemistry and were interpreted together with particle morphology and XRD-based mineral identification.

2 Supplementary data interpretation

2.1 Aluminium concentration in both bays

Dissolved Al in seawater (32-130 nmol/kg across both sites) was substantially lower than in freshwater (864 nmol/kg at Gåsbreen; Table 1). Hansbukta exhibited ~2-4-fold higher dAl than Gåshamna, indicating stronger lithogenic inputs. Concentrations peaked in the surface layer and declined with depth (Fig. S.4). Seasonal patterns were modest: Gåshamna showed higher dissolved Al in summer than in spring, whereas Hansbukta displayed only weak seasonal variability. Aluminium displayed a clear mixing-driven pattern across both Gåshamna and Hansbukta, with a pronounced negative relationship between dissolved Al and salinity during summer ($\rho = -0.62$, Table S.6), stronger than for the full dataset and consistent at both sites individually. Concurrently, summer conditions enhanced the coupling between Al and suspended particulate matter, particularly in Gåshamna, where Al vs. SPM correlations were notably elevated ($\rho = 0.68$, Table S.6), a pattern also evident, though weaker, when all summer data were pooled ($\rho = 0.44$). This indicates that seasonal increases in particulate export amplify the lithogenic imprint on aluminium distributions.

2.2 Macronutrients, particulate and dissolved carbon and nitrogen

Nutrient concentrations (DIN and PO_4^{3-}) were generally higher in spring (May) and declined in summer (July–August) (Fig. S.7), whereas particulate organic matter (POC and PTN) exhibited higher median values and greater variability during summer. Significant seasonal differences ($p < 0.05$) were observed only for DOC at both Hansbukta and Gåshamna, while other parameters (DIN, DSi, POC, PTN, δ^{13}C-POC, δ^{15}N-PTN) showed no consistent seasonal variability; PO_4^{3-} also showed no seasonal difference at Gåshamna. Spatially, Hansbukta displayed greater variability, particularly in summer, whereas Gåshamna showed higher spring nutrient concentrations. Between-site differences were significant for DOC, DIN, and DSi in summer, and for PO_4^{3-} in spring. Relationships with salinity (Fig. S.8) were generally weak for DOC and DIN, except for a modest positive trend for DIN in Hansbukta during summer. PO_4^{3-} and DSi showed more variable but occasionally significant positive relationships with salinity, particularly in Hansbukta (spring) and Gåshamna (summer for PO_4^{3-}; both seasons for DSi), suggesting partial coupling to freshwater inputs. In contrast, POC and PTN decreased with increasing salinity, with the strongest negative relationships in Hansbukta during spring indicating strong association with suspended particulate matter. Stable isotopes showed minimal dependence on salinity, with no significant trends for δ^{13}CPOC and only a marginal relationship for δ^{15}NPTN in Gåshamna during spring. The distribution of nutrients and organic matter suggests that DIN and PO_4^{3-} are primarily controlled by biological uptake and recycling rather than conservative mixing, whereas DSi and particulate matter are more strongly linked to freshwater inputs and weathering-derived material. This pattern highlights the importance of particle transport and glacial inputs in regulating Fe and Mn cycling, particularly in the tidewater system, while DOC dynamics appear to be governed by local production, transformation, and complexation processes.

2.3 Marine snow and flocculation

The fate of sediment-bound micronutrients is directly linked to flocculation processes because it is determining whether these elements are buried locally or transported offshore. Field observations from Kongsfjorden (Svalbard) show that fine suspended sediments delivered with meltwaters are rapidly transformed through flocculation at salinity gradients, where turbulence, particle concentration, and ionic strength jointly promote aggregation and increase settling velocities (Meslard et al., 2018) . These processes result in distinct “flocculation fronts” (Syvitski et al., 2026) along stratification gradients, as is visible through particle and marine snow fluxes at inner stations of Hornsund and not in Gåshamna (Fig. S.9). Most probably the observed plumes of suspensions are created by rapid growth of mineral-rich aggregates by flocculation that was enhanced at freshwater–seawater interface and by the presence of particle-rich layers. The fluxes assessed by the underwater optical counting and camera were of similar order of magnitude in Gåshamna between spring and summer, but much higher in summer in Hansbukta (too high to provide reliable estimates, because the suspended matter totally blinded the light source). If we assume that the particulate iron is incorporated into those aggregates, then it would mean that it is rapidly removed by sedimentation near glacier termini (Fig. S.9). However, its persistence in specific water layers rather than constant increase towards the sea floor may suggest that they may be buoyant and prone to horizontal transport (Markussen et al., 2016). However, as the outermost station did not show such accumulation of particle and marine snow fluxes, it would mean that the flocculation is local, and that the labile forms may be bonded to aggregates inside the bay, and stay apart and bioavailable for phytoplankton outside. Studies from West Greenland

demonstrate that flocculation of meltwater particles governs the transport and fate of labile iron, linking aggregation dynamics directly to the bioavailability of this key micronutrient in coastal waters (Markussen et al., 2016). The join analyses of suspended matter, particles, marine aggregates and micronutrients suggest that further studies are needed to better recognize the importance of flocculation as a central coupling mechanism between physical mixing and biogeochemistry, regulating how glacier-derived sediments and micronutrients are partitioned between rapid sedimentation and wider ocean export under ongoing climate-driven increases in meltwater discharge.

3 Supplementary figures

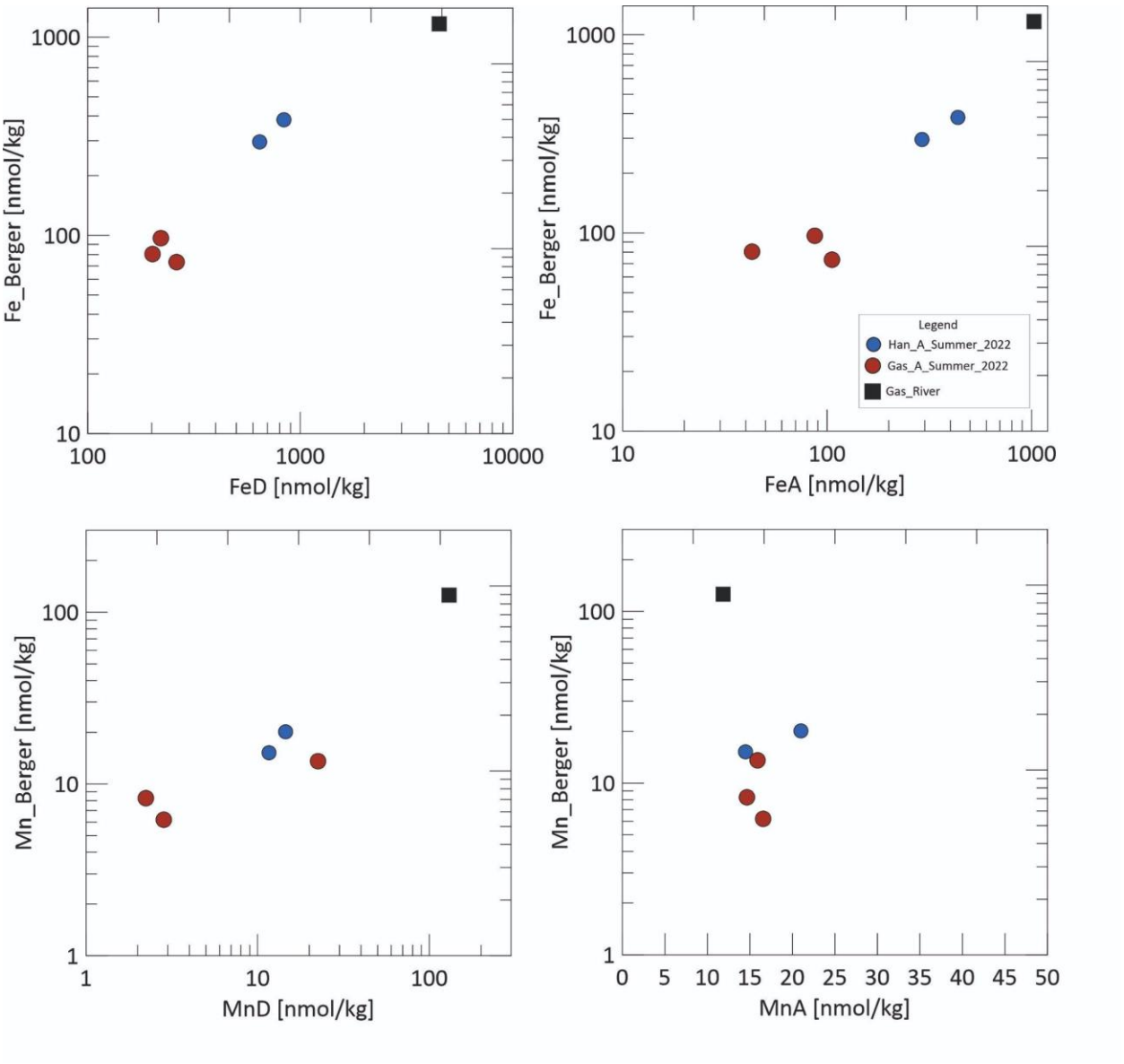

Fig. S.1. Comparison between content sediment-bound Fe (FeA, FeD) and Mn (MnA, MnD) and Berger leach in 2022.

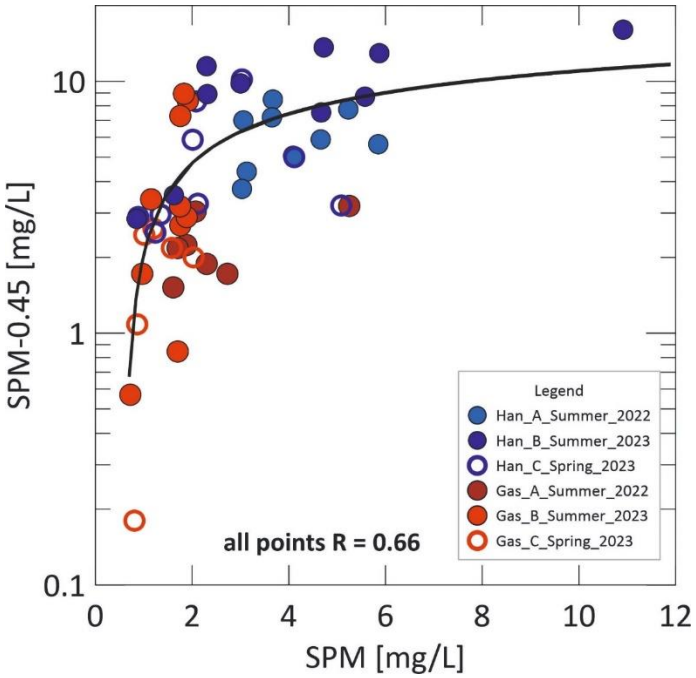

Fig. S.2. Relationship between SPM filtered by PES filters with pore size 0.45 um (SPM-0.45) and by GF/F with pore size 0.7 um (SPM) in Hansbukta and Gashamna.

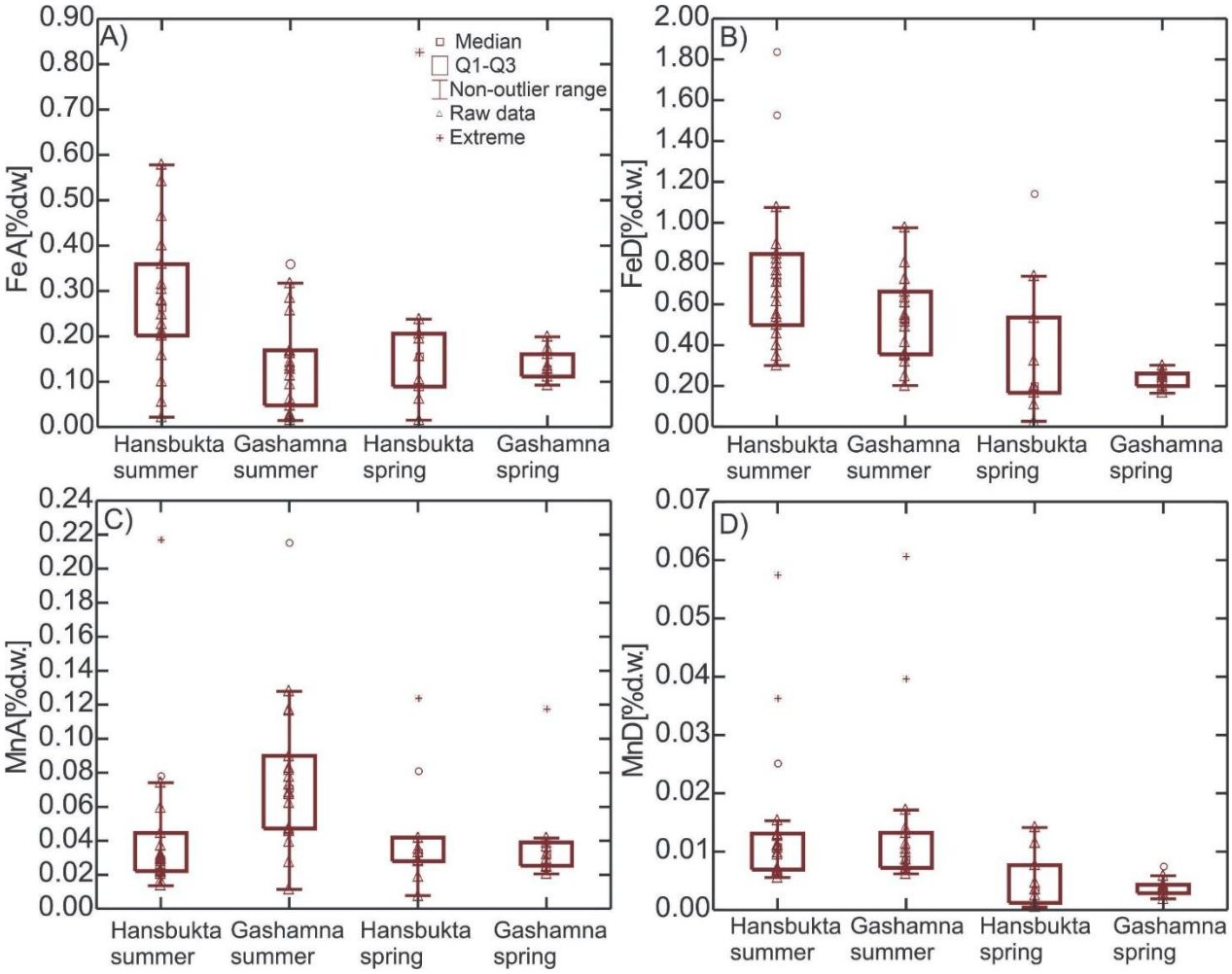

Fig. S.3. Sediment-bound Fe and Mn standarized for SPM concentration in Hansbukta and Gashamna in both summer seasons of 2022 and 2023 and spring season 2023. A) FeA [% d.w.], B) FeD [% d.w.], C) MnA [% d.w.], D) MnD [% d.w.].

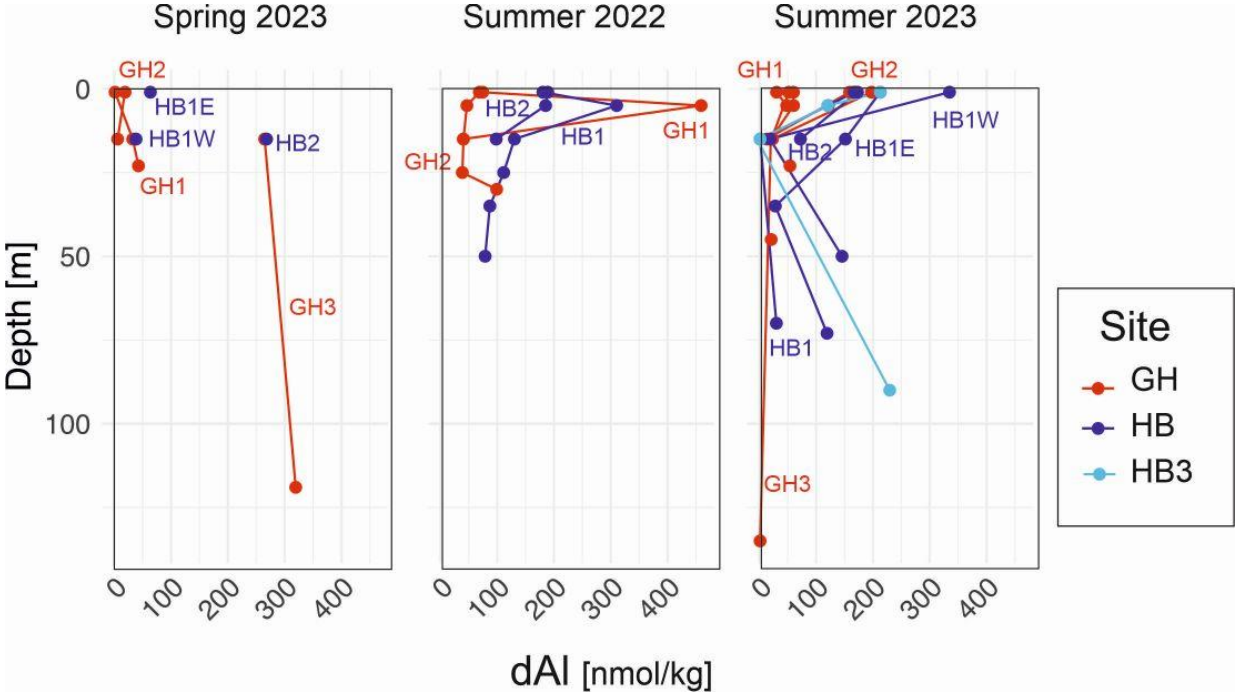

175

Fig. S.4. Dissolved Al in the water column in Hansbukta and Gashamna.

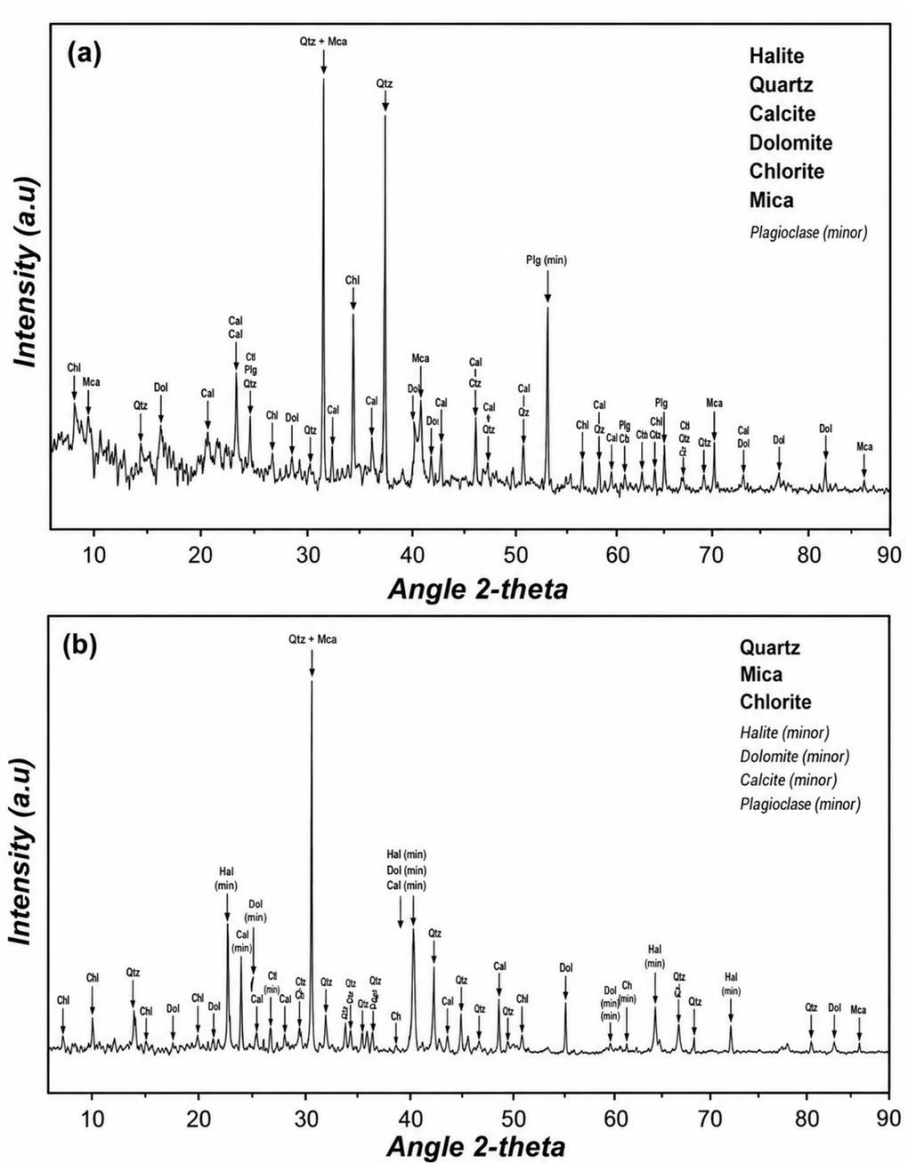

Figure S.5. X-ray diffraction patterns of suspended particulate matter from (a) Gashamna and (b) Hansbukta, Hornsund fjord, Svalbard. Peak labels indicate the main crystalline phases identified from the diffraction patterns. The Gashamna sample contains halite, quartz, calcite, dolomite, chlorite and mica, with plagioclase as a minor phase. The Hansbukta sample is dominated by quartz, mica and chlorite, with halite, dolomite, calcite and plagioclase present as minor phases. Abbreviations: Qtz - quartz; Mca - mica; Chl - chlorite; Cal - calcite; Dol - dolomite; Hl/Hal - halite; Plg/Pg - plagioclase. Halite is not part of the mineral composition in the SPM but a result of salt formation from seawater during sample preparation**.**

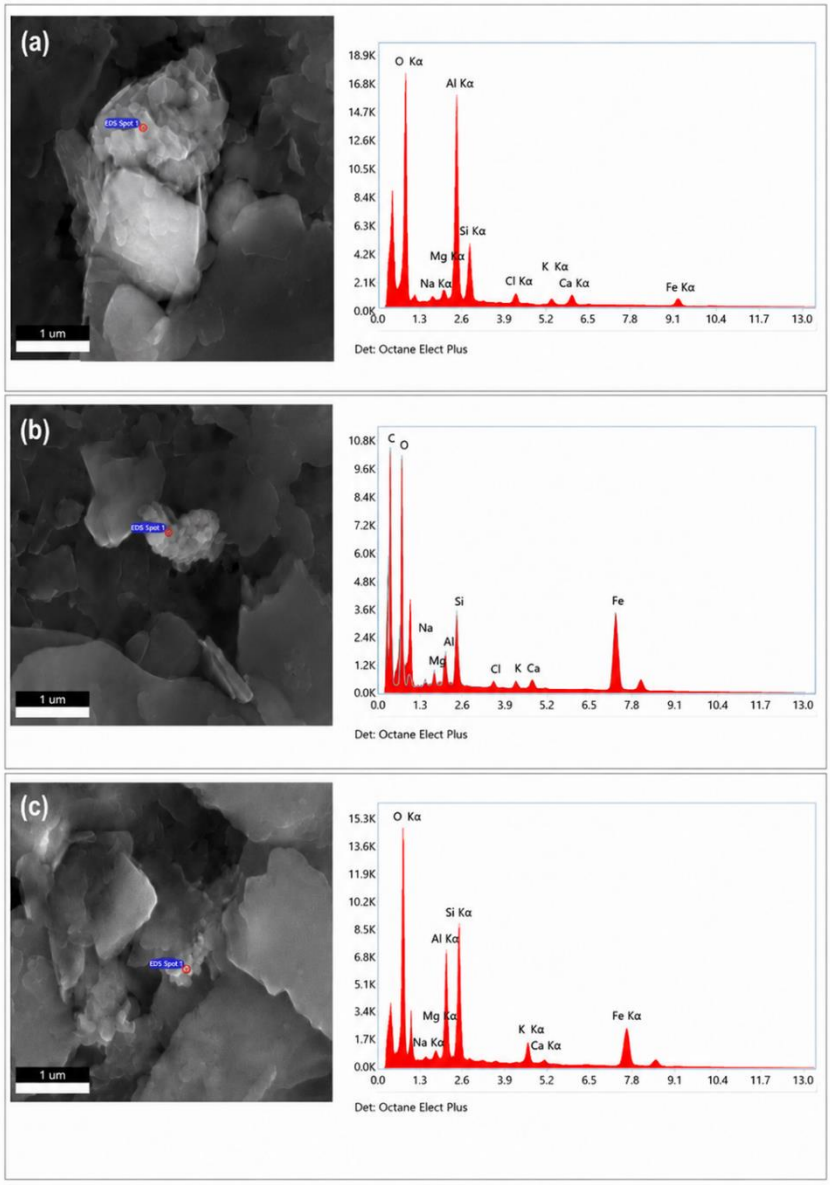

Figure S.6. SEM micrographs and corresponding EDS spectra of selected poorly ordered Fe-bearing particles and coatings in suspended particulate matter from the Hansbukta system. Panels (a-c) show different areas in SPM samples. EDS spectra indicate variable Fe enrichment associated with O-, Al- and Si-bearing particles and coatings. The spectra support the presence of fine-grained Fe-bearing material within glacial SPM, but chemistry and morphology from SEM-EDS is not adequate for identifying Fe-phases and therefore these particles are referred to as poorly ordered Fe-bearing phases.

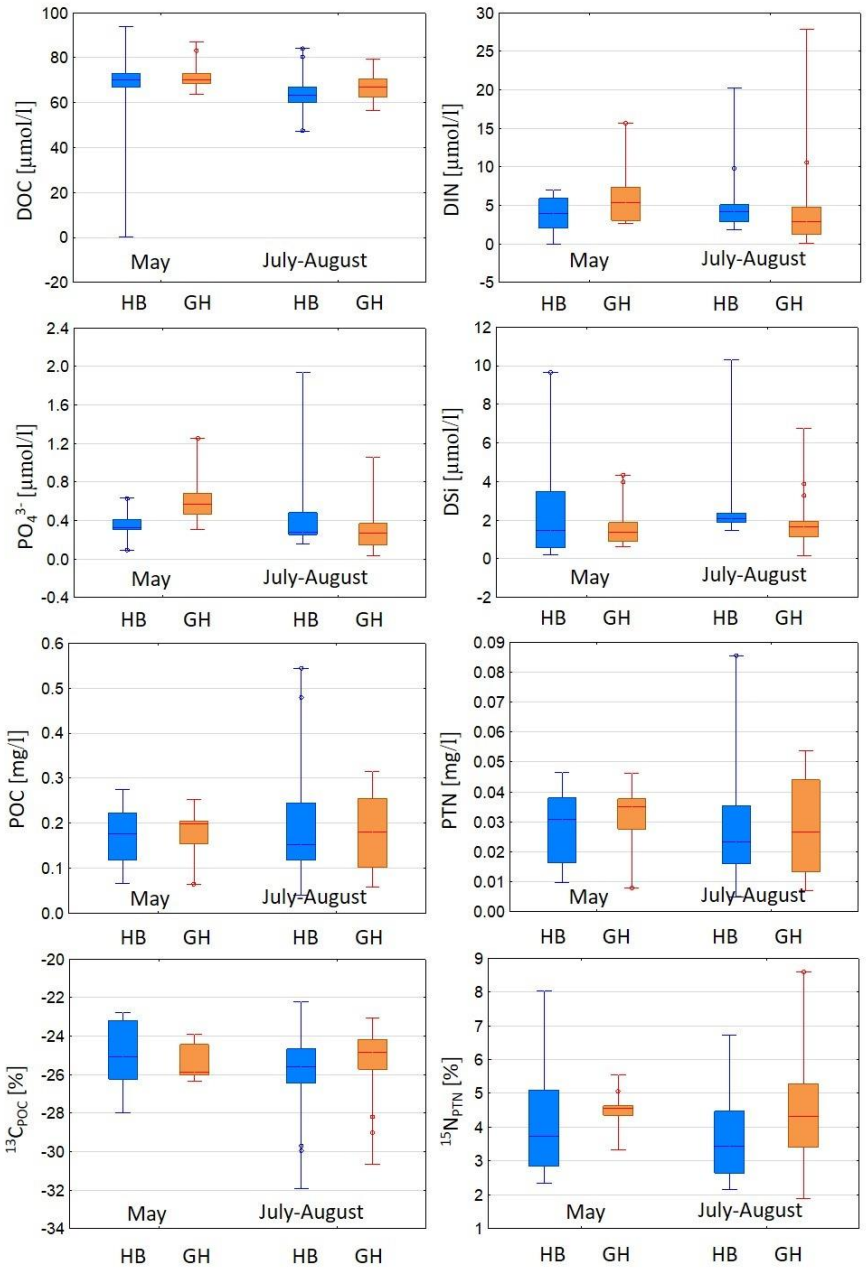

Fig. S.7. Box plots of dissolved organic carbon (DOC), nutrients (dissolved inorganic nitrogen (DIN, expressed as the sum of nitrate (NO_3^-), nitrite (NO_2^-), ammonium (NH_4^+), phosphate (PO_4^{3-})), particulate organic carbon (POC), particulate total nitrogen (PTN) as well as stable carbon ($\delta^{13}C_{POC}$) and nitrogen ($\delta^{15}N_{PTN}$) isotopes composition in the water column in summer and spring seasons of 2023 in Hansbukta (HB) and Gashamna (GH). The line in each box shows the median value, whereas the boxes represent the lower and upper quartiles, and the whiskers represent the minimum and maximum value; circles represent outliers.

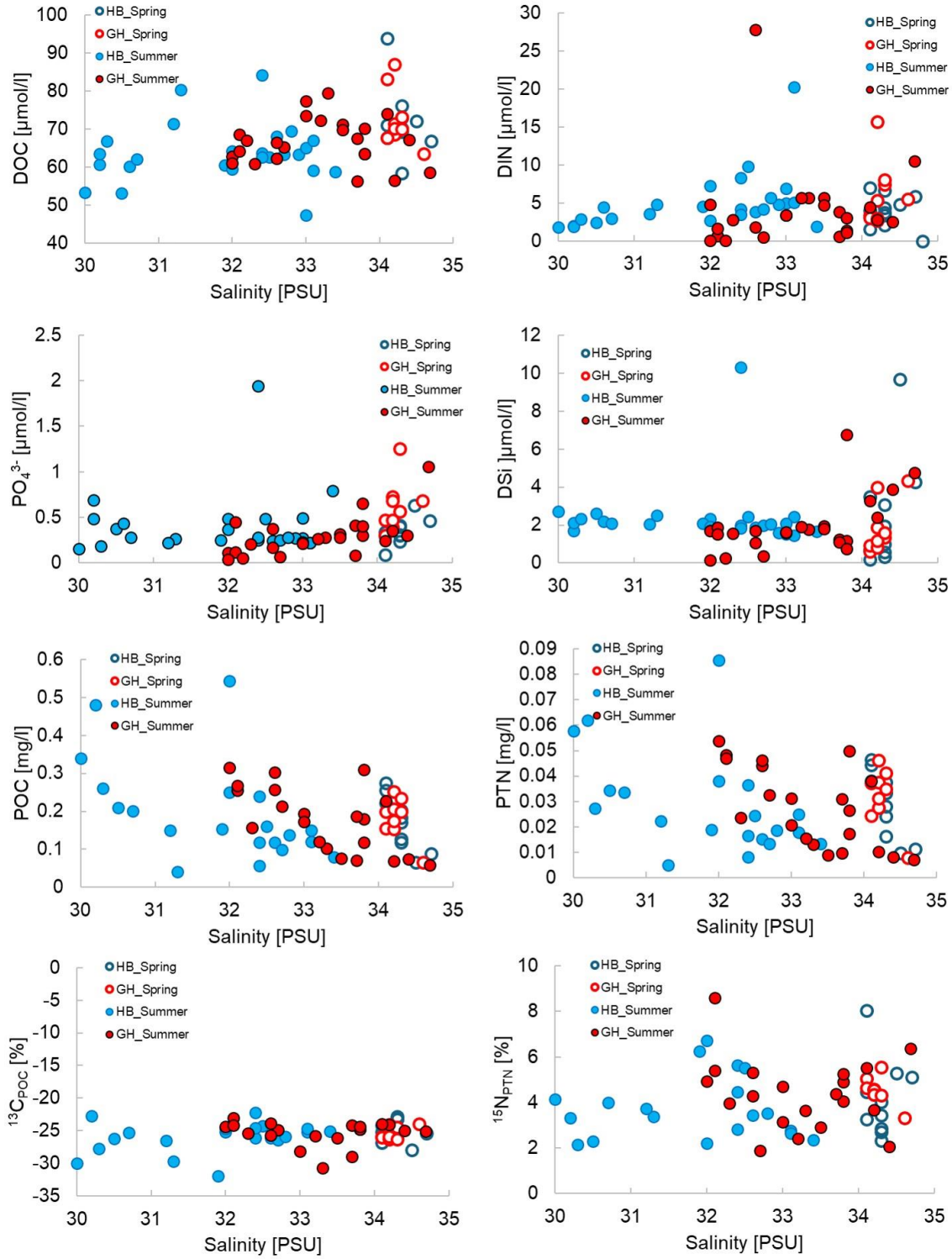

Fig. S.8. Relationship between salinity and dissolved organic carbon (DOC), nutrients (dissolved inorganic nitrogen (DIN, expressed as the sum of nitrate (NO_3^-), nitrite (NO_2^-), ammonium (NH_4^+), phosphate (PO_4^{3-}), particulate organic carbon (POC), particulate total nitrogen (PTN) as well as stable carbon ($\delta^{13}C_{POC}$) and nitrogen ($\delta^{15}N_{PTN}$) isotopes composition in the water column in summer and spring seasons of 2023 in Hansbukta (HB) and Gåshamna (GH).

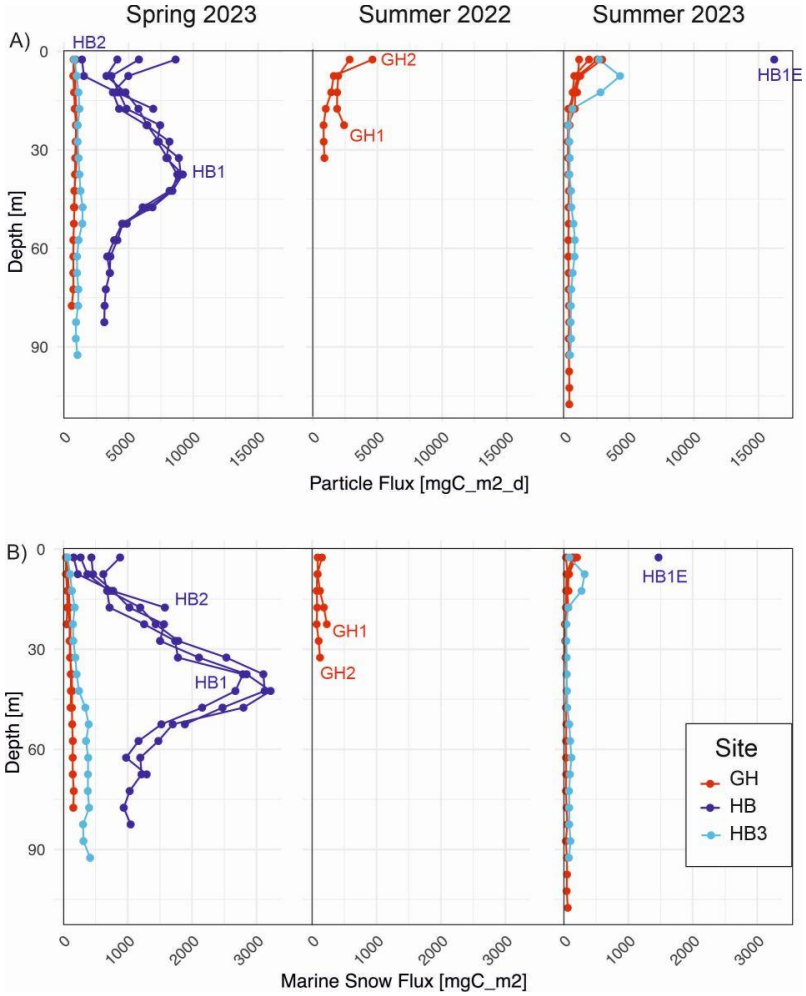

Fig. S.9. Fluxes of A) and marine snow (B) in spring and summer seasons assessed by UVP6 (Underwater Vision Profiler). For Hansbukta samples in both summer seasons of 2022 and 2023, measurements have not been conducted due to very high SPM concentration.

4 Supplementary tables

Table S.1. Instrumental operating parameters of the ICP–MS/MS (triple quadrupole) system, including plasma conditions, ion optics settings, and reaction cell parameters (NH_4 mode) used for the determination of Mn, Al, and Fe.

Parameter	Operating condition
RF Power (W)	1600
Nebuliser gas flow (L min^{-1})	0.87 – 0.92
Auxillary gas flow (L min^{-1})	1.2
AMS gas flow (L min^{-1})	0.1
Plasma gas flow (L min^{-1})	15
QID fixed voltage (V)	-18
Hyperskimmed parked voltage (V)	3 – 5
Omniring parked voltage (V)	4 – 6
Inner target lens voltage (V)	1 – 3.5
Outer target lens voltage (V)	-4 – -2.5
Ion Guide Mode	Focusing
Dwell time (ms)	50
Sweeps/Readings/Replicates	20.01.2003
Scan mode	NH_4 mode: MS/MS
Cell gas flow rate (mL min^{-1})	NH_4 mode: 0.6 (Mn, Al); 0.7 (Fe)
Mass selection (Q1/Q3)	Mn 55/55; Al 27/27; Fe 56/90
RPq	0.45
Nebulizer type	PFA OneTouch Microflow self-aspirating nebulizer
Nebulizer flow rate (µL min-1)	~100
Spray chamber type	SilQ Cyclonic Spray Chamber with Matrix Gas Port
Spray chamber temperature (°C)	4

220

Table S.2. Comparison of measured and certified concentrations of Fe, Mn, and Al in certified reference materials (SLEW-4, CASS-6, NASS-7) analysed by ICP–MS. Values are reported as mean ± standard deviation (n = replicates).

Element	SLEW-4		CASS-6		NASS-7	
	Measured	Certified	Measured	Certified	Measured	Certified
Fe (nmol L^{-1})	117.8 ± 8.1 (n = 23)	123.4 ± 8.6	28.8 ± 2.2 (n = 20)	27.9 ± 2.1	9.90 ± 2.08 (n = 11)	6.29 ± 0.47
Mn (nmol L^{-1})	75.3 ± 5.1 (n = 23)	74.6 ± 10.0	40.2 ± 3.0 (n = 20)	40.4 ± 2.2	13.4 ± 1.8 (n = 15)	13.5
Al (nmol L^{-1})	272.3 ± 16.5 (n = 23)	none	123.6 ± 13.1 (n = 20)	none	22.6 ± 6.3 (n = 10)	none

Table S.3. Total dissolvable (acidified unfiltered samples) concentration of Fe (TdFe), Mn (TdMn), Al (TdAl) in nmol/kg in water samples collected from Hansbukta and Gashamna ("mean, median (min-max)") in 2022 and 2023.

Parameter [nmol/kg]	Hansbukta (N=5)	Gåshamna (N=5)	River (N=1)
TdFe	3914.2, **2212.5** (231.5-10120.2)	560, **512.8** (353.9-1027.8)	20583.7
TdMn	116.9, **128.1** (17.8-249.8)	77, **100.4** (23.9-118.7)	814.3
TdAl	3943.4, **2658.5** (180.9-9039.4)	540.8, **621.9** (234.1-874.2)	11600.3

Table S.4. Geochemical indices of sediment-bound and dissolved trace elements (mean, median (min-max)).

Index	Hansbukta summer	Gåshamna summer	Hansbukta spring	Gåshamna spring	River
FeA:dFe*	12.2, **6.2** (0.7-35.6)	2.2, **1.7** (0.2-9)	3.5, **2.5** (1.3-6.8)	1.6, **2.1** (0.3-2.7)	2475, **2253.4** (33.9-5137.8)
FeA:FeD*	0.38, **0.4** (0.06-0.67)	0.27, **0.26** (0.03-0.82)	0.67, **0.53** (0.18-1.41)	0.6, **0.56** (0.37-0.86)	0.11, **0.08** (0.06-0.23)
FeD:dFe*	34.9, **21.7** (1.2-86.9)	8.7, **8.6** (2.4-22.8)	6, **7.8** (0.9-9.3)	2.9, **2.9** (0.6-6.8)	16131.4, **22525** (476.9-25392.2)
FeD:Al_D*	6.5, **6.5** (4-10.3)	6, **5.4** (2.4-11.1)	8.5, **5.7** (2.2-47.6)	8.7, **5.7** (3.3-19.6)	9.1, **9.6** (7.4-9.8)
dFe:dAl*	0.28, **0.17** (0.04-1.05)	0.58, **0.3** (0.08-2.17)	0.32, **0.33** (0.24-0.38)	0.96, **0.56** (0.08-2.38)	0.08, **0.08** (0.02-0.13)
MnA:Mn diss*	0.55, **0.25** (0.11-2.87)	0.67, **0.36** (0.14-3.6)	0.9, **0.83** (0.75-1.12)	0.68, **0.63** (0.39-1.56)	12.3, **2** (0.1-34.8)
MnA:MnD*	4.4, **3.5** (0.5-22)	8.3, **8.1** (0.7-24.8)	11.2, **8.8** (4.3-26.4)	9.9, **9.8** (6.7-15.5)	0.91, **0.91** (0.09-1.72)
MnD:dMn*	0.13, **0.11** (0.03-0.43)	0.15, **0.07** (0.02-0.73)	0.1, **0.11** (0.05-0.14)	0.07, **0.06** (0.04-0.11)	7.82, **2.43** (0.83-20.21)
MnD:Al_D*	0.12, **0.09** (0.07-0.48)	0.11, **0.11** (0.05-0.19)	0.11, **0.09** (0.03-0.49)	0.14, **0.12** (0.05-0.27)	0.17, **0.16** (0.08-0.28)
dMn:dAl*	0.97, **0.73** (0.05-3.67)	1.14, **1.09** (0.13-2.31)	0.24, **0.27** (0.05-0.41)	0.68, **0.36** (0.03-2.5)	0.1, 0.07 (0.06-0.18)
dMn:dFe*	6.3, **4.5** (0.3-25.7)	3, **2.2** (0.5-6.5)	0.72, **0.7** (0.22-1.25)	0.78, **0.79** (0.15-1.6)	2.12, **2.12** (0.56-3.68)
FeA**	0.28, **0.26** (0.02-0.58)	0.14, **0.13** (0.01-0.36)	0.21, **0.16** (0.02-0.83)	0.14, **0.13** (0.09-0.2)	0.17, **0.12** (0.04-0.4)
MnA**	0.04, **0.03** (0.01-0.22)	0.08, **0.07** (0.01-0.22)	0.04, **0.03** (0.01-0.12)	0.04, **0.03** (0.02-0.12)	0.03, **0.02** (0-0.09)
FeD**	0.76, **0.71** (0.3-1.84)	0.53, **0.53** (0.2-0.97)	0.38, **0.2** (0.03-1.14)	0.23, **0.24** (0.16-0.3)	2.09, **1.14** (0.49-5.6)
MnD**	0.015, **0.011** (0.006-0.057)	0.014, **0.009** (0.006-0.061)	0.005, **0.003** (0-0.014)	0.004, **0.004** (0.002-0.008)	0.04, **0.02** (0.01-0.1)

* - unit [nmol/kg:nmol/kg]

** - unit [% d.w.], based on standardisation by SPM concentration

Table S.5. Spearman's rank correlation coefficients (p < 0.05 are marked with red colour) for all sampling points, Gashamna and Hansbukta excluding freshwater samples. Concentrations are in nmol/kg excluding salinity (PSU).

Parameter	Type	dFe	FeA	FeD	dMn	MnA	MnD	dAl	Al._D	Salinity	SPM
dFe	All	1.00	0.20	0.05	-0.01	-0.24	0.14	0.35	-0.02	0.15	-0.08
FeA	All	0.20	1.00	0.80	0.60	0.26	0.73	0.37	0.68	-0.44	0.67
FeD	All	0.05	0.80	1.00	0.83	0.37	0.90	0.44	0.90	-0.79	0.76
dMn	All	-0.01	0.60	0.83	1.00	0.22	0.71	0.50	0.80	-0.83	0.73
MnA	All	-0.24	0.26	0.37	0.22	1.00	0.44	0.14	0.49	-0.30	0.14
MnD	All	0.14	0.73	0.90	0.71	0.44	1.00	0.32	0.91	-0.70	0.66
dAl	All	0.35	0.37	0.44	0.50	0.14	0.32	1.00	0.40	-0.45	0.39
Al._D	All	-0.02	0.68	0.90	0.80	0.49	0.91	0.40	1.00	-0.77	0.77
Salinity	All	0.15	-0.44	-0.79	-0.83	-0.30	-0.70	-0.45	-0.77	1.00	-0.63
SPM	All	-0.08	0.67	0.76	0.73	0.14	0.66	0.39	0.77	-0.63	1.00
dFe	Gas	1.00	0.24	0.29	0.01	-0.06	0.26	0.50	0.07	-0.03	0.08
FeA	Gas	0.24	1.00	0.60	0.22	-0.21	0.47	0.18	0.01	-0.33	0.47
FeD	Gas	0.29	0.60	1.00	0.73	0.25	0.85	0.47	0.77	-0.80	0.84
dMn	Gas	0.01	0.22	0.73	1.00	0.30	0.62	0.45	0.80	-0.85	0.70
MnA	Gas	-0.06	-0.21	0.25	0.30	1.00	0.48	0.06	0.66	-0.31	0.15
MnD	Gas	0.26	0.47	0.85	0.62	0.48	1.00	0.37	0.83	-0.72	0.71
dAl	Gas	0.50	0.18	0.47	0.45	0.06	0.37	1.00	0.44	-0.46	0.50
Al._D	Gas	0.07	0.01	0.77	0.80	0.66	0.83	0.44	1.00	-0.73	0.75
Salinity	Gas	-0.03	-0.33	-0.80	-0.85	-0.31	-0.72	-0.46	-0.73	1.00	-0.63
SPM	Gas	0.08	0.47	0.84	0.70	0.15	0.71	0.50	0.75	-0.63	1.00
dFe	Hans	1.00	0.27	0.15	0.03	-0.28	0.28	0.29	0.07	0.21	0.04
FeA	Hans	0.27	1.00	0.85	0.62	0.42	0.86	0.38	0.82	-0.61	0.63
FeD	Hans	0.15	0.85	1.00	0.70	0.36	0.96	0.38	0.94	-0.86	0.62
dMn	Hans	0.03	0.62	0.70	1.00	-0.11	0.66	0.45	0.60	-0.76	0.39
MnA	Hans	-0.28	0.42	0.36	-0.11	1.00	0.42	0.25	0.36	-0.26	0.15
MnD	Hans	0.28	0.86	0.96	0.66	0.42	1.00	0.28	0.90	-0.79	0.58
dAl	Hans	0.29	0.38	0.38	0.45	0.25	0.28	1.00	0.32	-0.49	0.19
Al._D	Hans	0.07	0.82	0.94	0.60	0.36	0.90	0.32	1.00	-0.85	0.63
Salinity	Hans	0.21	-0.61	-0.86	-0.76	-0.26	-0.79	-0.49	-0.85	1.00	-0.63
SPM	Hans	0.04	0.63	0.62	0.39	0.15	0.58	0.19	0.63	-0.63	1.00

Table S.6. Spearman's rank correlation coefficients (p < 0.05 are marked with red colour) for all samplng points, Gashamna and Hansbukta excluding freshwater samples and samples collected in spring 2023. Concentrations are in nmol/kg excluding Salinity (PSU).

Parameter	Type	dFe	FeA	FeD	dMn	MnA	MnD	dAl	Al._D	Salinity	SPM
dFe	All	1.00	0.23	0.12	0.05	-0.34	0.29	0.23	0.04	0.12	-0.08
FeA	All	0.23	1.00	0.91	0.59	-0.11	0.78	0.43	0.81	-0.58	0.81
FeD	All	0.12	0.91	1.00	0.75	-0.07	0.82	0.56	0.93	-0.75	0.88
dMn	All	0.05	0.59	0.75	1.00	-0.14	0.54	0.66	0.72	-0.75	0.70
MnA	All	-0.34	-0.11	-0.07	-0.14	1.00	-0.28	0.05	0.07	-0.08	-0.18
MnD	All	0.29	0.78	0.82	0.54	-0.28	1.00	0.37	0.91	-0.51	0.82
dAl	All	0.23	0.43	0.56	0.66	0.05	0.37	1.00	0.49	-0.62	0.44
Al._D	All	0.04	0.81	0.93	0.72	0.07	0.91	0.49	1.00	-0.70	0.91
Salinity	All	0.12	-0.58	-0.75	-0.75	-0.08	-0.51	-0.62	-0.70	1.00	-0.68
SPM	All	-0.08	0.81	0.88	0.70	-0.18	0.82	0.44	0.91	-0.68	1.00
dFe	Gas	1.00	0.31	0.44	0.04	-0.32	0.45	0.31	0.14	-0.09	0.10
FeA	Gas	0.31	1.00	0.73	0.09	-0.60	0.60	0.20	-0.16	-0.22	0.46
FeD	Gas	0.44	0.73	1.00	0.44	-0.50	0.76	0.61	0.49	-0.65	0.71
dMn	Gas	0.04	0.09	0.44	1.00	-0.04	0.26	0.66	0.78	-0.67	0.70
MnA	Gas	-0.32	-0.60	-0.50	-0.04	1.00	-0.41	-0.29	0.24	0.12	-0.44
MnD	Gas	0.45	0.60	0.76	0.26	-0.41	1.00	0.45	0.57	-0.48	0.71
dAl	Gas	0.31	0.20	0.61	0.66	-0.29	0.45	1.00	0.63	-0.66	0.68
Al._D	Gas	0.14	-0.16	0.49	0.78	0.24	0.57	0.63	1.00	-0.49	0.78
Salinity	Gas	-0.09	-0.22	-0.65	-0.67	0.12	-0.48	-0.66	-0.49	1.00	-0.51
SPM	Gas	0.10	0.46	0.71	0.70	-0.44	0.71	0.68	0.78	-0.51	1.00
dFe	Hans	1.00	0.36	0.29	0.11	-0.28	0.45	0.21	0.19	0.15	0.06
FeA	Hans	0.36	1.00	0.94	0.54	-0.09	0.86	0.44	0.92	-0.68	0.70
FeD	Hans	0.29	0.94	1.00	0.58	-0.10	0.94	0.46	0.93	-0.69	0.62
dMn	Hans	0.11	0.54	0.58	1.00	-0.46	0.53	0.52	0.45	-0.68	0.24
MnA	Hans	-0.28	-0.09	-0.10	-0.46	1.00	-0.24	0.28	0.04	-0.11	-0.10
MnD	Hans	0.45	0.86	0.94	0.53	-0.24	1.00	0.32	0.82	-0.53	0.53
dAl	Hans	0.21	0.44	0.46	0.52	0.28	0.32	1.00	0.41	-0.62	0.20
Al._D	Hans	0.19	0.92	0.93	0.45	0.04	0.82	0.41	1.00	-0.73	0.64
Salinity	Hans	0.15	-0.68	-0.69	-0.68	-0.11	-0.53	-0.62	-0.73	1.00	-0.49
SPM	Hans	0.06	0.70	0.62	0.24	-0.10	0.53	0.20	0.64	-0.49	1.00

References

Berger, C.J.M., Lippiatt, S.M., Lawrence, M.G., Bruland, K.W., 2008. Application of a chemical leach technique for estimating labile particulate aluminum, iron, and manganese in the Columbia River plume and coastal waters off Oregon and Washington. 113(C2). https://doi.org/10.1029/2007JC004703

Forsch, K.O., Ruacho, A., Aarons, S.M., 2025. Tidewater cycle drives alpine glacial sediment plume geochemistry. 16(1). 10.1038/s41467-025-64731-1

Grasshoff, K., Kremling, K., Ehrhardt, M., 2009. Methods of seawater analysis. John Wiley & Sons, Weinheim New York Chichester Brisbane Singapore Toronto.

Markussen, T.N., Elberling, B., Winter, C., Andersen, T.J., 2016. Flocculated meltwater particles control Arctic land-sea fluxes of labile iron. 6, 24033. 10.1038/srep24033

Meslard, F., Bourrin, F., Many, G., Kerhervé, P., 2018. Suspended particle dynamics and fluxes in an Arctic fjord (Kongsfjorden, Svalbard). 204, 212-224. https://doi.org/10.1016/j.ecss.2018.02.020

Saghravani, S.R. et al., 2024. Distributions of in situ parameters, dissolved (in)organic carbon, and nutrients in the water column and pore waters of Arctic fjords (western Spitsbergen) during a melting season. 16(7), 3419-3431. 10.5194/essd-16-3419-2024

Syvitski, J. et al., 2026. Inorganic mineral flocculation within mid-to-high latitude deep coastal basins. 491, 107675. https://doi.org/10.1016/j.margeo.2025.107675